

Photovoltaic Array Modelling and Boost-Converter Controller-Design for a 6kW Grid-Connected Photovoltaic System - DC Stage

Noureddin Motan
Birzeit University
 Birzeit, Palestine
 nmotan@gmail.com

Muhammad Abu-Khaizaran
Birzeit University
 Birzeit, Palestine
 mkhaizaran@birzeit.edu

Mahran Quraan
Birzeit University
 Birzeit, Palestine
 mquraan@birzeit.edu

Abstract—Grid-connected Photovoltaic (PV) systems have increased dramatically in the last few years due to the increased global interest in renewable energy sources and the growth in energy demand. Consequently, new and modern control strategies should be applied to improve the efficiency, reliability, and stability of grid-connected PV systems. To achieve this, the whole PV system should be tested under various weather and grid conditions. However, the wide variety of the PV system devices and control algorithms, in addition to the destructive nature of many types of scenarios and faults, make the practical testing of the PV system very difficult, very expensive, and impossible in many cases. Therefore, this paper utilizes the modelling and simulation tools of Matlab/Simulink to develop an accurate model for a grid-connected PV system-DC stage.

The developed model implements all components of the grid-connected PV system at the DC side; these components are a PV array, a Boost converter, and a Maximum Power Point Tracking (MPPT) controller. Each component of the system is modelled, simulated and validated. Then the PV system is used to simulate many scenarios under various grid and weather conditions. The simulation results show that the model is reliable, stable and suitable for studying the grid-connected PV system.

Index Terms—Grid Connected, Maximum Power Point Tracker (MPPT), Photovoltaic (PV), and Voltage Source Inverter (VSI)

I. INTRODUCTION

THE tremendous increase in energy demand, the growth of global interest in renewable and clean energy sources, and the advances in research and technology in solar Photovoltaic (PV), all led to significant advances in PV industry. For instance, the PV cost benchmark for residential PV systems in U.S. decreased from \$7.24/Wdc in 2009 to \$2.8/Wdc in 2017, as shown in Fig. 1 [1]. Moreover, Fig. 2 shows that the PV energy production soared from below 10GW in 2006 to more than 300GW in 2016. In addition, during 2016, more than 75GW of solar PV capacity was added worldwide, compared to 50GW in 2015 [2]–[4]. According to [5] “the Compound Annual Growth Rate (CAGR) over the last 15 years was above 40%, which makes PV one of the fastest growing industries at present”.

PV systems can be classified into two major categories: grid-connected PV systems and off-grid (stand-alone) PV

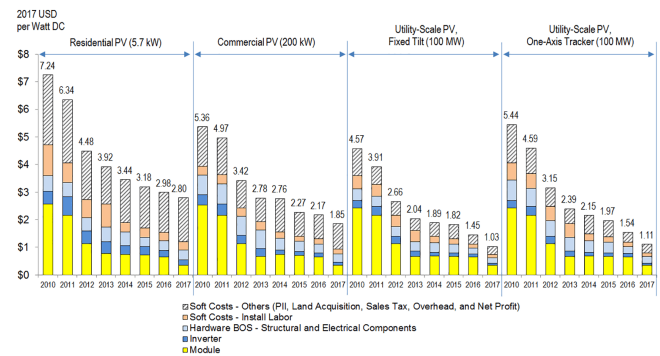


Fig. 1. PV system cost benchmark summary [1]

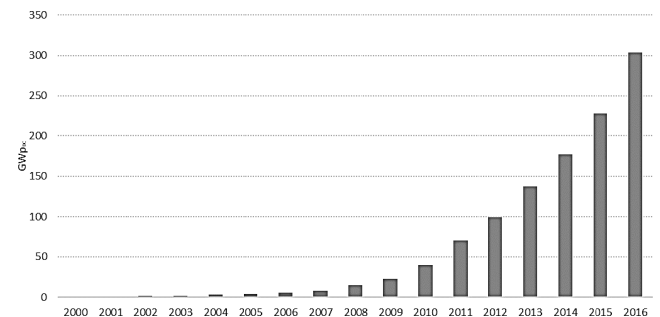


Fig. 2. Evolution of PV installation [2]

systems. The grid-connected PV systems operate in parallel with electric grid to increase the output power of the grid, while off-grid systems have no connection to the electric grid. Off-grid systems are used in some applications such as roof-mounted PV system, solar vehicle, solar powered lamps, and water pumps [6]. Nowadays, the vast majority of PV systems are grid-connected, while off-grid applications represent only 1% of the market, down from more than 90% two decades ago [7].

Fig. 3 shows a typical grid-connected system. Typically, it consists of a PV array, a Maximum Power Point Tracking (MPPT) Controller, a DC-DC converter, a DC-AC inverter, grid interface, control unit, and protection interfacing [6].

In this paper, modelling and simulation of a PV array, Boost

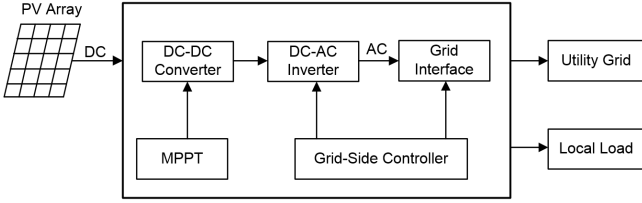


Fig. 3. A typical grid-connected PV system

DC-DC converter, and the MPPT algorithm controller are presented. The model of the PV array is presented, simulated, and validated against a PV cell datasheet. A closed loop controller for the Boost converter is designed such that, it provides a regulated DC voltage at the Boost converter's output, and simultaneously operates the PV array at the MPP of any weather condition. Finally, conclusions are drawn and summarized.

II. PV SYSTEM MODELLING

A. Modelling a Photovoltaic Cell

A Photovoltaic (PV) array is composed of a large number of PV modules. Each module consists of a group PV cells connected in series and in parallel. A particular PV cell is made of semiconductor material that produces a DC voltage/current when exposed to sunlight [8].

The basic component of a PV system is the PV cell. Therefore, in order to study and design the whole PV system, it is important to construct a model for the PV cell. A reliable and an accurate mathematical model of PV cell is important to design and simulate other parts of the PV system and to design the control algorithms of the PV system. This model is also useful in studying and designing the MPPT algorithm, the Boost converter, and the control strategy and the synchronization algorithm. Moreover, datasheets of the PV modules provide the module parameters at Standard Test Condition (STC) only. Thus, the mathematical model uses that information to predict the device's behavior at any condition accurately.

Various models of the PV were proposed, varying in complexity and accuracy; ranging from ideal models to practical models [9], [10]. The practical PV model takes into account the leakage current, the internal resistance and wiring resistance. The practical PV model is depicted in Fig. 4 (a).

Since a PV module is constructed from several PV cells connected in series and in parallel combinations, the voltage-current relationship for the PV module is given by:

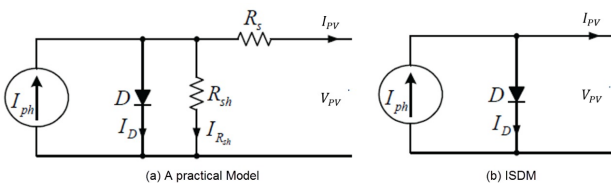


Fig. 4. A PV cell models

$$I_{PV} = I_{ph} - I_s \left[e^{\left(\frac{q(V_{PV} + I_{PV}R_s)}{N_s A k T} \right)} - 1 \right] - \frac{V_{PV} + I_{PV}R_s}{R_{sh}} \quad (1)$$

where, I_{PV} is the current output of a PV cell, V_{PV} the PV voltage, I_{ph} is the photo current (depends on the solar irradiance (G) and cell temperature (T)), I_s is the diode saturation current, q is the electron charge, k is the Boltzmann constant, T is the PV cell temperature in Kelvin, A is the diode ideality constant, N_s is the number of series connected cells, R_s is the equivalent series resistance of the module and R_{sh} is the equivalent parallel resistance.

The Ideal Single Diode Model (ISDM) approach of a PV cell proposed by Mahmoud et al. [11], which is simple, efficient and needs less simulation time than other models, has been modelled using Matlab/Simulink. This model is developed to estimate the equivalent circuit parameters of ISDM shown Fig. 4 (b). The Matlab/Simulink model of the PV module has been used in the simulation of the PV system constructed. Hence, eq. (1) can be further simplified to be expressed as eq. (2), which relies on the ISDM:

$$I_{PV} = I_{ph} - I_s \left[e^{\left(\frac{qV_{PV}}{N_s A k T} \right)} - 1 \right] \quad (2)$$

I_{ph} in eq. (2) is determined as follows [11]:

$$I_{ph} = G(I_{SC} + \alpha \Delta T) \quad (3)$$

where G the solar irradiance (kW/m^2), I_{SC} is the short circuit current at STC, which is given in the datasheet, ΔT is the difference between the module temperature and the STC temperature ($25^\circ C$), and α is the current temperature coefficient provided in the product datasheet. Neglecting R_s and R_{sh} and evaluating eq. (2) at STC ($G = 1$ and $T = 25^\circ C$) and $V_{ph} = V_{OC}$ yield:

$$I_{rs} = \frac{I_{SC}}{\left[e^{\left(\frac{qV_m}{N_s k A T_o} \right)} - 1 \right]} \quad (4)$$

where I_{rs} is the saturation current at STC.

By evaluating eq. (2) at STC and the Maximum Power Point (MPP), I_{rs} can be further expressed as [11]:

$$I_{rs} = \frac{I_{SC} - I_m}{\left[e^{\left(\frac{qV_m}{N_s k A T_o} \right)} - 1 \right]} \quad (5)$$

Equations (4) and (5) can be solved to get the diode ideality factor, A [11].

To find the I_s :

$$V_{OC}(G, T) - V_{OC}(G, T_o) = -|\beta| \Delta T \quad (6)$$

where $V_{OC}(G, T)$ is the open circuit voltage at given temperature and irradiance levels, $V_{OC}(G, T_o)$ is the open circuit voltage at STC temperature ($25^\circ C$) and irradiance, β is the temperature coefficient of V_{OC} (given in the datasheet) [11]. By substituting $I_{PV} = 0$ in (2), the open circuit voltage formula is determined as [11]:

$$V_{OC}(G, T) = \frac{N_s k T A}{q} \ln \left(\frac{I_{ph}}{I_s} + 1 \right) \quad (7)$$

Substituting eq. (3) in eq. (7) yields:

$$V_{OC}(G, T) = \frac{N_s k T A}{q} \ln\left(\frac{G(I_{SC} + \alpha \Delta T)}{I_s} + 1\right) \quad (8)$$

By evaluating eq. (8) at T and T_o and substituting in eq. (6) yield:

$$\frac{N_s k A}{q} [T \ln\left(\frac{G(I_{SC} + \alpha \Delta T)}{I_s} + 1\right) - T_o \ln\left(\frac{G I_{SC}}{I_s} + 1\right)] = -|\beta| \Delta T \quad (9)$$

By rearranging eq. (9), I_s can be expressed as:

$$I_s = \frac{I_{ph} e^{\left(\frac{|\beta| \Delta T q}{N_s k A T}\right)}}{\left(\frac{G I_{SC}}{I_s} + 1\right) \frac{T_o}{T} - e^{\left(\frac{|\beta| \Delta T q}{N_s k A T}\right)}} \quad (10)$$

B. Maximum Power Point Tracking (MPPT) Controller

The MPPT controller is an essential and a very important part in any PV system. It is used to extract the maximum power from the PV array. The output power of a PV array is influenced by solar irradiance and temperature. The output power of PV modules increases when the irradiance increases. It also increases when the temperature decreases. The function of the MPPT controller is to produce the control signal to the switch in the DC-DC converter, which controls the output voltage from PV module or array to ensure that the PV module or array supplies its maximum power to the system at any temperature and irradiance values. Many MPPT methods have been reported in the literature. These methods differ from each other regarding PV array dependency, implementation complexity, accuracy, and implementation cost [12], [13]. One of the most common MPPT techniques is the Hill Climbing or Perturb and Observe (P&O) method [14], [15]. The main advantages of this method is that it is independent of the PV array, it has a good performance, and it is easy to implement.

C. DC-DC Boost Converter

The Boost, or step-up converter, topology is commonly used in PV systems. The PV Array-Boost converter connection is shown in Fig. 5. The Boost converter is controlled using Pulse Width Modulation (PWM) control strategy. The generation of PWM control signals is achieved by implementing MPPT algorithm. For a continuous current conduction, the relationship between the PV array output voltage (V_{PV}) and the Boost converter voltage (V_o) is:

$$V_o = \frac{V_{PV}}{(1 - D)} \quad (11)$$

where D is the Duty cycle of the converter's switch.

III. SIMULATIONS AND VALIDATION

A. PV Characteristic Curves

Equations (4) to (10) were modelled in the Matlab/Simulink to determine the equivalent circuit parameters of KC200GT PV module [16]. The values of unknowns at STC were found as: $I_{ph} = 8.21A$, $I_s = 1.78 \times 10^{-5} A$, and $A = 1.82$. These parameters were inserted in a prepared Matlab/Simulink model to obtain the characteristics curves of the PV modules.

Fig. 6 shows the I-V characteristics of the PV module, consisting of 54 series cells, which are very similar to the actual behavior of a real PV module for different irradiance (G) levels. Whilst, Fig. 7 shows the I-V characteristics of the PV module for different temperatures (T), which are very close to the actual behavior of a real PV module under the same conditions.

Fig. 8 shows the P-V characteristics of the PV at a constant temperature and various levels of irradiance. It is clear that the output power of the PV modules increases when the irradiance increases. Fig. 9 shows the P-V characteristics of the PV at constant irradiance and different temperatures. It is clear from the figure that the output power of PV modules increases when the temperature decreases.

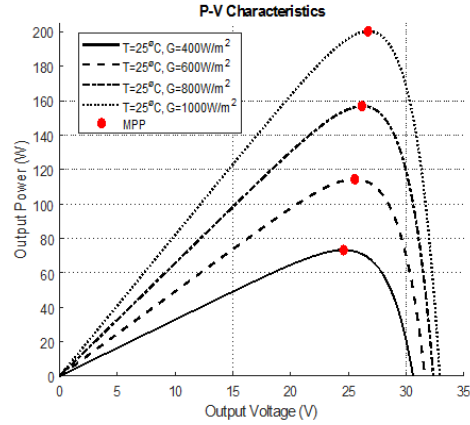


Fig. 8. P-V characteristic of the PV module at different G and a constant T

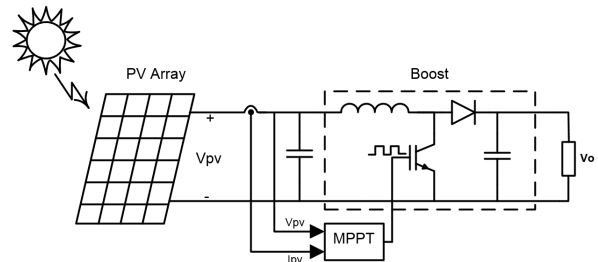


Fig. 5. PV Array-Boost converter connection

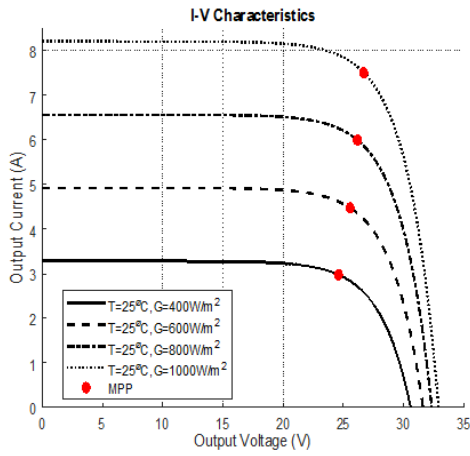


Fig. 6. I-V characteristic of the PV module at different G and a constant T

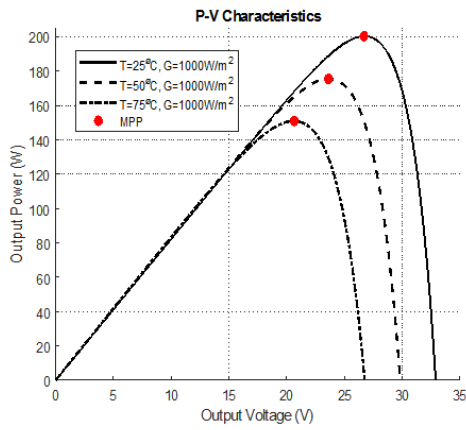


Fig. 9. P-V characteristic of the PV module at different T and a constant G

Fig. 10 and Fig. 11 show the datasheet I-V characteristics of the PV module [16]. By comparing the datasheet characteristics in Fig. 10 and Fig. 11 with those obtained by simulation in Fig. 6 and Fig. 7, it is obvious that the simulation results match well the characteristics of the PV module in the datasheet.

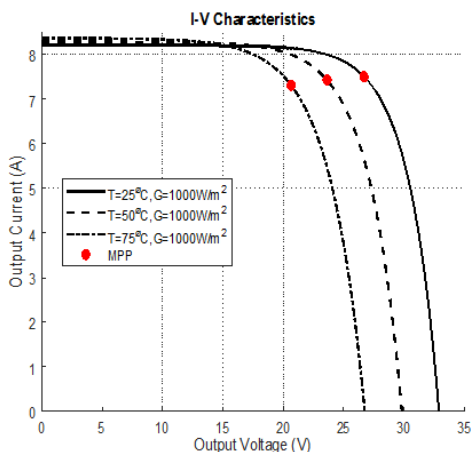


Fig. 7. I-V characteristic of the PV module at different T and a constant G

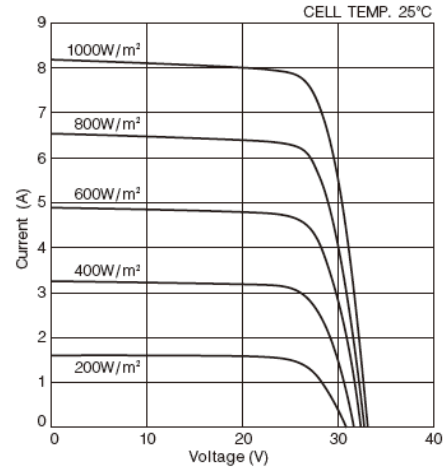


Fig. 10. I-V characteristic of the PV module as in datasheet at different irradiances, and $T = 25^\circ C$

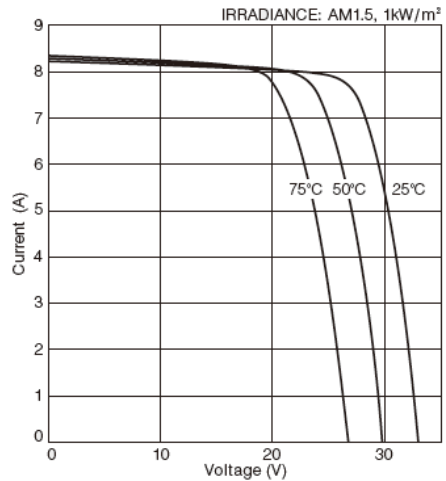


Fig. 11. I-V characteristic of the PV module as in datasheet at different temperatures, and $G = 1000 W/m^2$

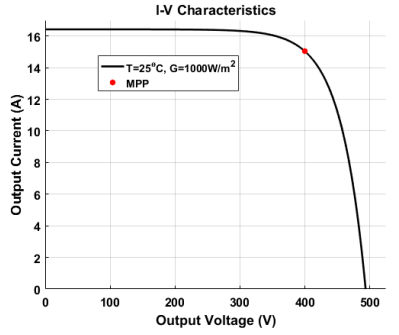
The model of the PV module can be expanded to model the PV array by setting the value of I_{PV} and V_{PV} in (2) as follows [17]:

$$I'_{PV} = p \cdot I_{PV} \quad (12)$$

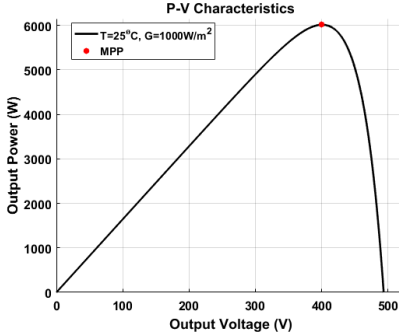
$$V'_{PV} = s \cdot V_{PV} \quad (13)$$

where s is the number of series modules, and p is the number of parallel modules.

The KC200GT module has a maximum power of 200Wp at STC. To get 6kW, a PV array was constructed by using 2 PV strings such that each of them consists of 15 series connected modules. The I-V and P-V characteristics curves at STC are shown in Fig. 12.



(a) I-V characteristic curve



(b) P-V characteristic curve

Fig. 12. PV array characteristic curves at STC

B. Boost Converter

The Boost converter Simulink model is shown in Fig. 13. It is designed to operate in a Continuous current Conduction Mode (CCM) using the following equations [18]:

$$L > \frac{D(1-D)^2 T_S V_o}{2I_o} \quad (14)$$

$$C = \frac{DT_S}{R \frac{\Delta V_o}{V_o}} \quad (15)$$

A closed loop control system for the Boost converter is designed implementing a PI controller, which is tuned using Matlab PID tuner.

The Boost converter is simulated with a variable magnitude reference voltage applied to its controller, and the output is observed. The result, shown in Fig. 14, indicates that the system is stable and has a zero-steady state error.

Another simulation is conducted by applying a variable input to the Boost converter and observing the output voltage, while keeping the reference voltage constant. The simulation

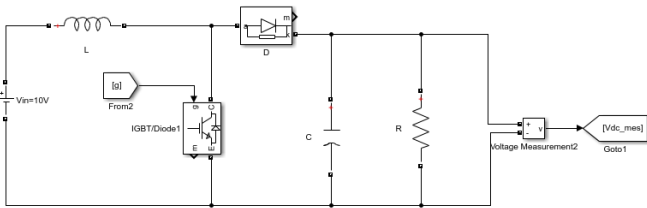


Fig. 13. The Boost converter's Simulink model

result is shown in Fig. 15. The result shows that the system is stable; its output voltage has a small steady state error for a ramp input, a fast response, and an overshoot for a step change in the input voltage.

C. MPPT Implementation

The MPPT controller, implementing Perturb and Observe (P&O) algorithm, is programmed in Matlab to control the duty cycle of the Boost converter's switch in order to extract the maximum power from the PV array. Fig. 16 shows the Simulink circuit used to test the MPPT algorithm.

Fig. 17 illustrates the operation of the MPPT controller and the Boost converter. It is clear that, when the MPPT controller is enabled at $t = 0.4s$, it controls the duty cycle of the Boost converter to operate the PV array at the maximum power point. In addition, by comparing the input voltage (V_{PV}) with the output voltage (V_o) in Fig. 17, the boosting action of the converter is obvious.

Another simulation test is done by applying variable temperature and irradiance to the PV array, and then measuring the output power from the PV array. Fig. 18 shows the simulated results. To validate the MPPT algorithm, the simulated results are compared with the data from the P-V characteristic of the PV module (Fig. 8 and Fig. 9). Clearly, the MPPT forces the system to operate at the maximum Power Point.

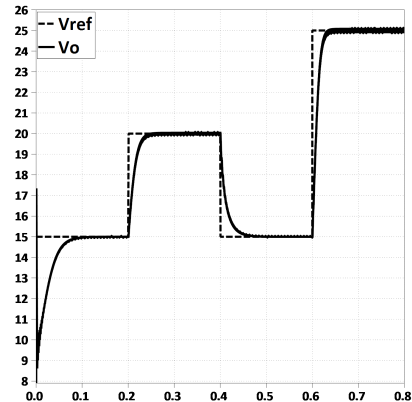


Fig. 14. The reference voltage and the output voltage of the Boost converter

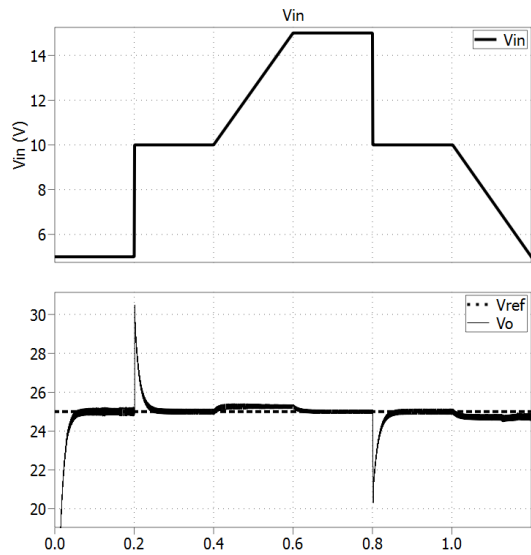


Fig. 15. The input, output and reference voltages of the Boost converter

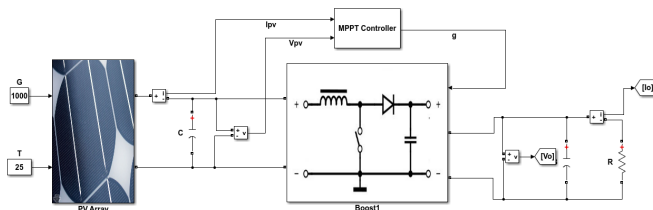


Fig. 16. The Simulink circuit to test the MPPT algorithm

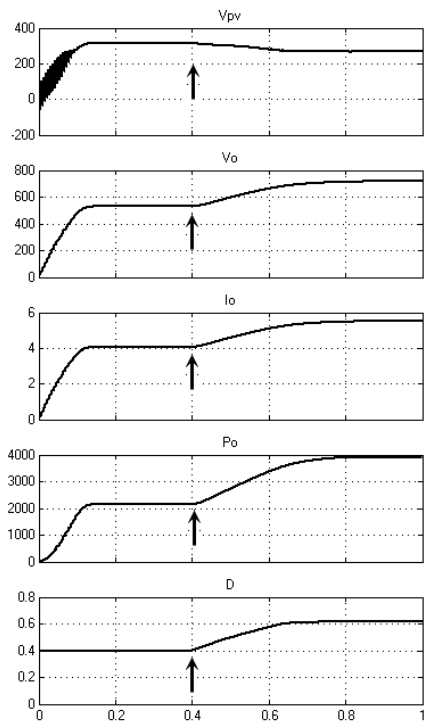
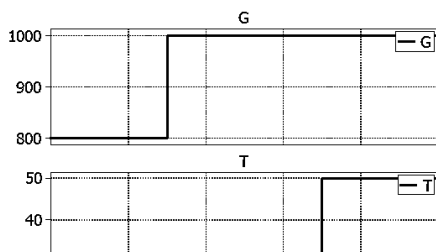


Fig. 17. Boosting and MPPT simulation results



IV. CONCLUSIONS

In this paper, modelling of a Photovoltaic array in Matlab/Simulink environment is presented. The PV Array model is simple and accurate as is shown in simulation results. The simulation results are validated against the datasheet of a real Photovoltaic module, and the simulation results match well the real Datasheet. Perturb and Observe algorithm for Maximum Power Point (MPP) tracking is implemented in Matlab to generate the appropriate PWM signals applied to the power electronic switch in the Boost converter. The significance of using the MMP tracking on the amount of the generated power is clearly seen in many simulation results. The Boost converter is operated in a closed loop such that, it operates the PV array at MPP, and also it provides a constant output DC voltage, 700V, which will be used for the inverter stage at varying weather conditions; in a work entitled “*Design and Modelling of a 6kW Grid-Connected Photovoltaic System-AC Stage*” [19].

REFERENCES

- [1] R. Fu, D. Feldman, R. Margolis, M. Woodhouse, and K. Ardani, “U.S. Solar Photovoltaic System Cost Benchmark: Q1 2017,” National Renewable Energy Laboratory (NREL), Tech. Rep., 2017.
- [2] IEA-PVPS, “2016 Snapshot of Global Photovoltaic Markets,” 2016.
- [3] IRENA, “Renewable Capacity Statistics 2017,” 2017.
- [4] REN21 Secretariat, “Renewables 2017 Global Status Report,” p. 302, 2017.
- [5] A. Jäger-Waldau, “PV Status Report 2016,” 2016.
- [6] M. Rashid, *Power Electronics Handbook*, 3rd ed. Elsevier, 2011.
- [7] REN 21 Steering Committee, “Renewables 2013 Global Status Report,” 2013.
- [8] M. R. Patel, *Wind and Solar Power Systems: Design, Analysis, and Operation*. CRC press, 2005.
- [9] M. G. Villalva, J. R. Gazoli, and E. R. Filho, “Comprehensive Approach to Modeling and Simulation of Photovoltaic Arrays,” *IEEE Transactions on Power Electronics*, vol. 24, no. 5, pp. 1198–1208, May 2009.
- [10] H.-L. Tsai, C.-S. Tu, and Y.-J. Su, “Development of Generalized Photovoltaic Model Using MATLAB/SIMULINK,” in *World Congress on Engineering and Computer Science*, 2008, pp. 0–5.
- [11] Y. Mahmoud, W. Xiao, and H. H. Zeineldin, “A Simple Approach to Modeling and Simulation of Photovoltaic Modules,” *IEEE Transactions on Sustainable Energy*, vol. 3, no. 1, pp. 185–186, Jan 2012.
- [12] T. Esmar and P. L. Chapman, “Comparison of Photovoltaic Array Maximum Power Point Tracking Techniques,” *IEEE Transactions on Energy Conversion*, vol. 22, no. 2, pp. 439–449, June 2007.
- [13] M. A. G. de Brito, L. Galotto, L. P. Sampaio, G. d. A. e Melo, and C. A. Canesin, “Evaluation of the Main MPPT Techniques for Photovoltaic Applications,” *IEEE Transactions on Industrial Electronics*, vol. 60, no. 3, pp. 1156–1167, March 2013.
- [14] D. Sera, L. Mathe, T. Kerekes, S. V. Spataru, and R. Teodorescu, “On the Perturb-and-Observe and Incremental Conductance MPPT Methods for PV Systems,” *IEEE Journal of Photovoltaics*, vol. 3, no. 3, pp. 1070–1078, July 2013.
- [15] S. E. Babaa, M. Armstrong, and V. Pickert, “Overview of Maximum Power Point Tracking Control Methods for PV Systems,” *Journal of Power and Energy Engineering*, vol. 02, no. 08, pp. 59–72, 2014.
- [16] Kyocera, “KC200GT High Efficiency Multicrystal Photovoltaic Module Datasheet,” 2009.
- [17] W. Xiao, F. F. Edwin, G. Spagnuolo, and J. Jatskevich, “Efficient Approaches for Modeling and Simulating Photovoltaic Power Systems,” *IEEE Journal of Photovoltaics*, vol. 3, no. 1, pp. 500–508, Jan 2013.
- [18] B. M. Hasaneen and A. A. E. Mohammed, “Design and Simulation of DC/DC Boost Converter,” in *2008 12th International Middle-East Power System Conference*, March 2008, pp. 335–340.
- [19] Anonymous, “Design and Modelling of a 6kW Grid-Connected Photovoltaic System-AC Stage,” in *IEEE International Conference on Environment and Electrical Engineering (EEEIC)*, under submission 2018.